C. R. Geoscience 348 (2016) 159–168

Contents lists available at ScienceDirect

Comptes Rendus Geoscience

www.sciencedirect.com

Tectonics, Tectonophysics

Structural geometry and kinematic processes at the intracontinental Daloushan mountain chain: Implications for tectonic transfer in the Yangtze Block interior

Bin Deng [a], Zhi-Wu Li [a,*], Shu-Gen Liu [a,*], Guo-Zhi Wang [a], Shuang-Jian Li [b], Zuo-Pen Qin [a], Jing-Xi Li [a], Luba Jansa [c]

[a] State Key Laboratory of Oil and Gas Reservoir Geology and Exploitation, Chengdu University of Technology, no. 1, 3rd ErxianQiao RD E, 610059 Chengdu, China
[b] Petroleum Exploration and Production Institute of SINPOEC, 10083 Beijing, China
[c] Dalhousie University, Halifax & Geological Survey of Canada-Atlantic, Dartmouth, N.S., Canada

ARTICLE INFO

Article history:
Received 24 March 2015
Accepted after revision 11 June 2015
Available online 13 August 2015

Handled by Isabelle Manighetti

Keywords:
Superimposed fold
Layer-parallel shortening
Apatite fission-track
Daloushan
Yangtze Block

ABSTRACT

The Daloushan mountain chain, located in the centre of the upper Yangtze continental block, is considered to represent the locus of the tectonic shortening resulting from the eastward growth of the Tibetan Plateau and NW-thrusting of the Xuefeng Orogen. Structural data and apatite fission-track ages have been used to decipher the geometry and the kinematic evolution of the Daloushan. The latter is subdivided into two domains: the eastern domain, governed by west- to NW-verging thrusting and deformation with dextral transpression, and a western domain, governed by south-verging thrusting and deformation. Both domains experienced four episodes of deformation, synchronous with the four stages of post-Cretaceous denudation, marked by rapid cooling propagating eastward from 20 to 5 Ma, at a rate of ~0.1 mm/year. In particular, the last two episodes of denudation are closely related to the growth of the Tibetan Plateau. This indicates an intra-continental transfer of tectonic forcing from the Palaeo-Pacific to the Tethys-Himalayan Tectonic Domain across the Daloushan.

1. Introduction

Mountain building processes record deformation at plate margins (e.g., the Andes and the Himalayas) and within continental interiors (e.g., the Tien Shan and the Pyrenees). However, how continental collision influences the mountain building within continental interiors remains a subject of controversy. A variety of processes has been suggested, such as continental homogeneity and strain localization (e.g., tectonic escape, channel flow; Royden et al., 2008; Tapponnier et al., 2001). The Daloushan (or Dalou Mountains) forms a distinct tectonic and morphologic boundary along the Sichuan Basin within the upper Yangtze Block. The mountain chain trends nearly east–west, with the locus of mountain building orthogonal to the continental margin (e.g., the Longmenshan and Qinling orogens; Fig. 1a). Thus, this region could provide clues for a better understanding of the evolution and geodynamics of intracontinental structures related to plate boundary deformation.

Two scenarios have been proposed to explain the deformation in the Daloushan. In the first one, post-Jurassic tectonics was interpreted to be the result of northwestward thrusting of the Xuefeng Orogen, in response to northwestward subduction of the Palaeo-Pacific Plate

* Corresponding authors.
E-mail addresses: lzw06@cdut.cn (Z.-W. Li), lsg@cdut.edu.cn (S.-G. Liu).

http://dx.doi.org/10.1016/j.crte.2015.06.009
1631-0713/

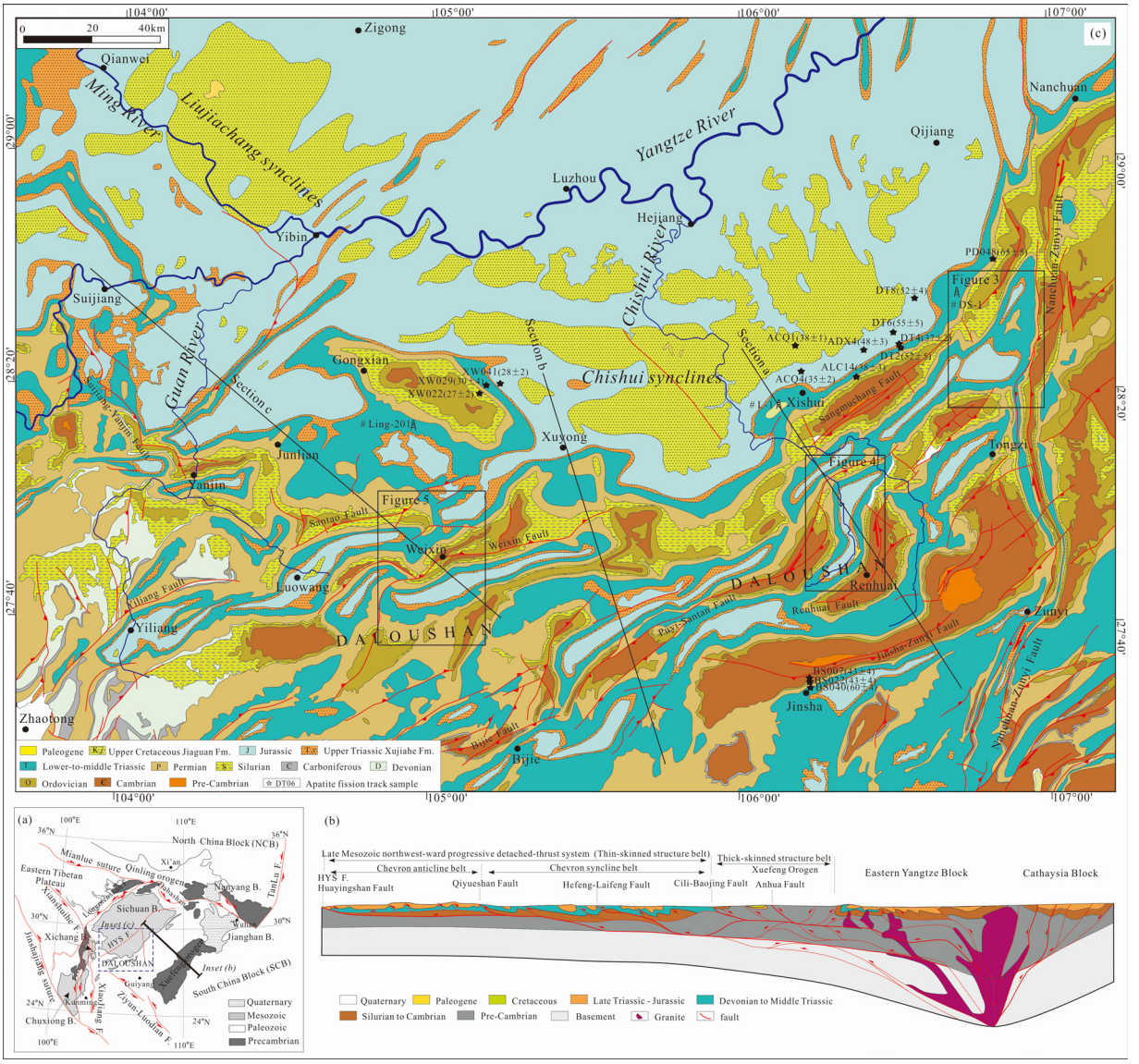

Fig. 1. (Color online) (a) Tectonic map of the South China Block with the location of the Daloushan. (b) Cross-section across the upper Yangtze Block. (c) Geologic map of the Daloushan based on field mapping and the published map of BGMRSP. Locations of apatite fission-track samples and cross sections (sections a, b, c) are shown.
Modified by Li et al. (2012) and Wang et al. (2013).

(Wang et al., 2013 and reference therein). In the second one, it is believed that a far-field effect of the India–Asia collision affected the entire Asian continent. It includes the eastward growth of the Tibetan Plateau (Roger et al., 2010; Royden et al., 2008) and the extrusion of the South China Block (SCB) (Lacassin et al., 1995; Leloup et al., 1995; Tapponnier et al., 2001). This geodynamic interaction resulted in a complex intra-continental deformation of the Asian continent. Both scenarios are possible; however, the details of structural and chronological constraints are too few to reach a definite conclusion.In this study, we use structural data and apatite fission-track ages to decipher geometry and kinematic evolution of the Daloushan. We arrive at the conclusion that this mountain belt is the main locus of deformation related to the northwestward thrusting of the Xuefeng Orogen, superimposed by eastward growth of the Tibetan Plateau. It should be noted that we use the term "eastward growth" for a complicated process of eastward expansion of the plateau, rather than for its mechanism.

2. Geologic setting

The South China Block (SCB) consists of the upper Yangtze Block in the northwest and the Cathaysian Block in the southeast (Fig. 1). To the north, the SCB is separated from the North China Block by the Qinling Orogen, and to the west, it is separated from the eastern Tibetan Plateau by the Longmen-Daliang Mountains. Two tectonic

processes affected the framework of the eastern Tibetan Plateau:

thrusting with sinistral strike-slip during the Late Triassic (Liu et al., 2012; Roger et al., 2010);

an east-west shortening during the Cenozoic (Lacassin et al., 1996; Roger et al., 2010). The latter is attributed to an eastward extrusion of crustal material from the Tibetan Plateau (Royden et al., 2008; Wilson et al., 2006).Within the SCB, the Sichuan Basin is separated from a 1300-km-wide Mesozoic intracontinental orogenic belt by the Qiyueshan-Daloushan Mountains. These mountains underwent a complicated tectono-magmatic evolution during the Late Mesozoic, referred to as the Yanshanian Intracontinental Orogeny (Hsu et al., 1990). Although still disputed, this orogeny has been generally linked to the westward low-angle subduction of the Palaeo-Pacific Plate (Li and Li, 2007).

2.1. Structures in the study area

The Daloushan displays NE- to NS-trending folds and thrusts, and regional NE- to NS-trending strike-slip faults (Fig. 1c). The tectonic style is characterized by Jura-style folds, which are considered to be controlled by the detachment along the Lower Cambrian and Lower Silurian strata (Liu et al., 2012; Yan et al., 2003). Some of the faults in the upper Yangtze Block were reactivated during the NW–NS Early Cretaceous extension related to lithospheric extension (Li and Li, 2007), and during the NS–NW post-Cretaceous compression, producing gentle folds much different from the underlying strata, which is dominated by chevron and box folds (BGMRSP, 1991).

2.2. Stratigraphic succession of the Yangtze Block

The upper Yangtze Block consists of up to 10 km of Neoproterozoic–Phanerozoic strata, comprised mainly of Palaeozoic and Middle Mesozoic shallow-marine deposits, as well as post-Late Triassic terrestrial deposits. Most of the Upper Silurian, Devonian and Carboniferous strata are absent, due to the Caledonian movement across the Yangtze Block. Mesozoic angular unconformities (e.g., J_2/K_1) become younger, fewer and weaker from the eastern side of the Xuefeng Orogen to the Daloushan, where a paraconformity is visible (BGMRSP, 1991). In particular, significant uplift and erosion has occurred since the Late Paleogene (Deng et al., 2013; Li et al., 2012a, 2012b, 2012c), resulting in a restricted occurrence of Cenozoic rocks in the upper Yangtze Block. The Lower Cenozoic rocks show similar fluvial-lacustrine facies across the southern Sichuan basin and its periphery. They are reliably dated in several places to Early Cenozoic, having a conformable contact with the underlying strata (BGMRSP, 1991; Deng et al., 2012). Neogene rocks are even more restricted than the Lower Cenozoic rocks, and have an unconformable contact with the other strata.

3. Structural analysis

To constrain the geometry of the Daloushan, most of these regions were mapped at a 1:100,000 scale, and combined with field surveys. Three oil exploratory wells provided additional control on the depth and thickness of the Phanerozoic sedimentary series (Fig. 1). This allowed the construction of three NW–SE sections across the Daloushan (Fig. S1). Cross-sections A and B cut through the eastern and middle segments of the Daloushan, exhibiting the dominant presence of north-vergent thrusts and Jura-style folds. In contrast, section C shows south-verging thrusts and Jura-style folds at the western segment.Due to multiphase shortening, there is some uncertainty about the shortening magnitude across these three sections. Therefore, we simply restored these cross-sections through area balancing of the Paleozoic sequence using AreaErrorProp software (Judge and Allmendinger, 2013). This shows that the shortening amount of the Xishui-Renhuai, Xuyong-Dafang, and Weixin-Suijiang cross-sections are 19.1 ± 3.1 km (i.e. $\sim 12.3 \pm 2.2\%$), 11.9 ± 3.7 km (i.e. $8.8 \pm 3.2\%$) and 11.7 ± 3.3 km (i.e. $9.0 \pm 3.6\%$), indicating a westward decrease of the shortening.

3.1. Eastern Nanchuan-Tongzi area

The eastern segment of the Daloushan is cut by the north-south-striking Nanchuan-Zunyi Fault (Fig. 1c and 2), characterized by westward thrusting and dextral strike-slipping. Folds resemble the Jura-type and reflect the NW- to east–west-trending shortening. However, most of the bedding surfaces and joints in the Triassic–Jurassic strata show a marked dispersion (Fig. 2a), typical of multiple deformations.

The superimposed folds resulting from multiphase deformation are common in many deformed areas (e.g., Yelang and Songkan). In the Nanchuan-Tongzi area, the D_1 deformation is characterized by isoclinal folds of metric wavelength and amplitude (Fig. S2a), with gently NE- to NNE-plunging axes and upright, or steeply inclined axial planes. It indicates an east–west- to WNW-oriented shortening. The axes and the axial planes were refolded by the subsequent D_2 folds (Fig. S2a). These are characterized by open to tight folds of decametric to hectametric wavelength and amplitude, and upright, or steeply inclined axial surfaces. More than 60 bedding attitude data points (S_0) from superimposed folds plot along two great circles, indicating two different orientations of shortening (Fig. S2b). The poles are coincident with the D_1 and D_2 axes. This suggests that the F_1 axis of the D_1 deformation resulted from nearly east–west-oriented shortening, and that the F_2 axis of D_2 deformation resulted from northeast- to NNE-oriented shortening.

Two types of sub-vertical, or bedding-perpendicular joint sets were recognized in the eastern segment. A carefully back-rotated inversion was executed by checking with the Anderson stress model, assuming that the maximum stress was nearly horizontal, when the bedding planes were horizontal. At most studied sites, a single rotation about bed strike, which was assumed to be parallel to the fold axis, was used for restoration. For sites located along plunging folds, the plunge was first removed, followed by a rotation about the partly restored bedding strike. The first set of joints is orthogonal to bedding, with moderate to subvertical dips and a NW–SE or NE–SW trend (Fig. 2b). The maximum palaeostress of conjugated joints suggests the presence of an

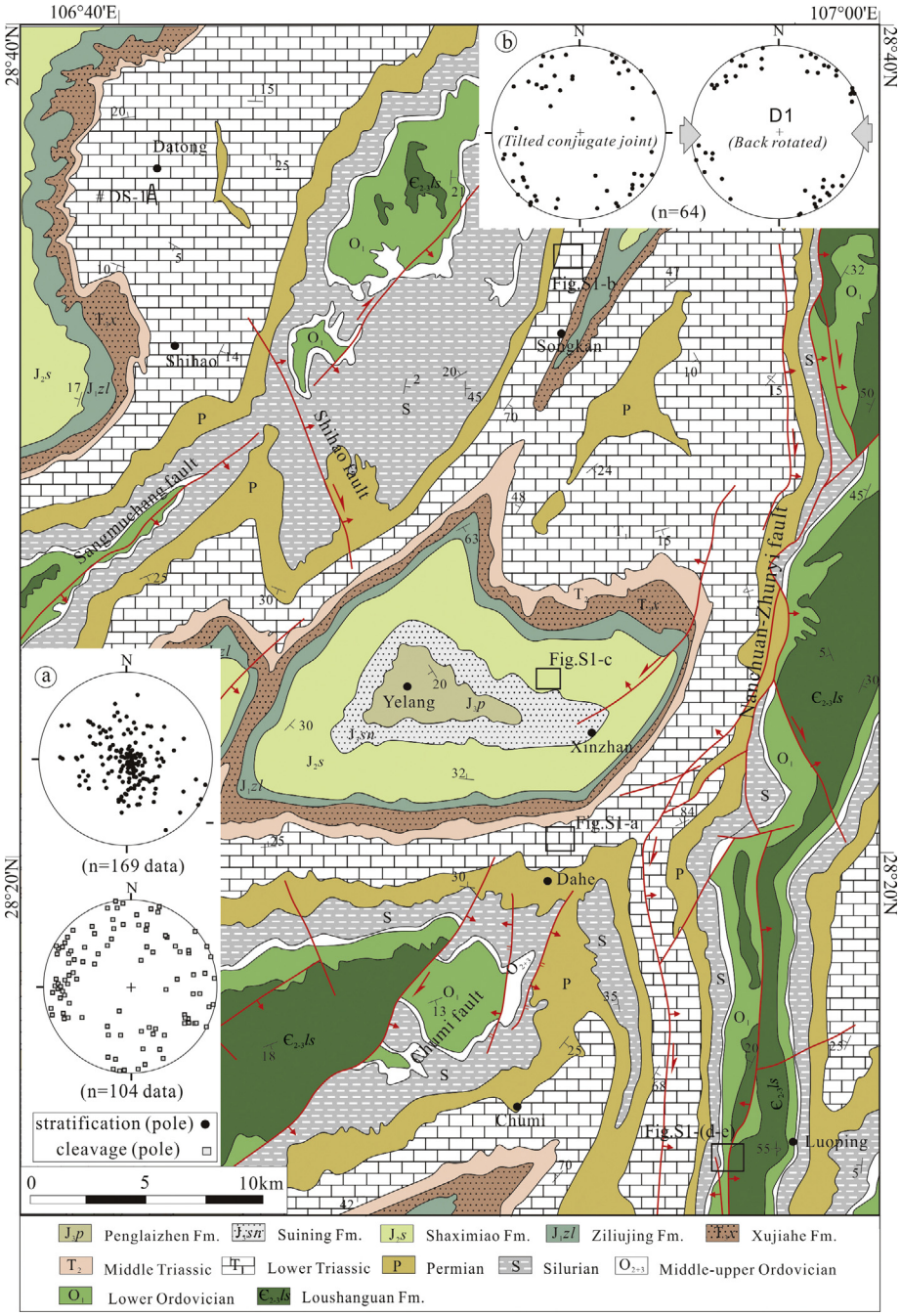

Fig. 2. (Color online) Detailed geologic map and representative structures of the eastern part of the Daloushan. (a) Dispersed stratification and cleavage in region, indicating multiple deformations. (b) *In situ* and back-rotated conjugate joint sets, indicating an east–west-trending parallel-layer shortening (D_1). The trend of σ_1 is shown. All data are projected in an equal area stereogram, lower hemisphere.

east–west-oriented (D_1) deformation. Cross-cutting and abutting relations indicate that this is the oldest conjugate set. Accordingly, D_1 represents the oldest deformation event. Note that the east–west-oriented shortening of bedding-perpendicular joints is roughly coeval with low-angle, or layer-parallel fault-slip in some places. The second set of joints that locally developed results from D_2 folds that are subvertical to the northeast or the northwest. After back-rotation, they show a high-angle, or sub-perpendicular orientation to structural trends (Fig. 2c), indicating a south–north-oriented shortening deformation.

The eastern segment is associated with south–north- to NNE-trending west-to-NW-oriented thrusts (Fig. 2). To the south, the hanging wall of the Nanchuan-Zunyi Fault consists of overturned Cambrian strata. The pervasive cleavage at the core of folds is dominant with 115° ∠ 76° (i.e. dip-direction and dip angle), indicating a west-vergent thrusting shear (Fig. S2d). Furthermore, minor faults and

fault-slips show distinct dextral thrusting under nearly east–west-oriented shortening (Fig. S2e). In general, fault planes of the Nanchuan-Zunyi Fault, with characteristic striations and para-folds are widespread, and exhibit west-vergent thrusting with dextral transpression.

3.2. Middle Xishui-Renhuai area

Superimposed folds are common along the dextral shear in the middle segment. The D_2 folds are isoclinal folds and have metric to decametric wavelength and amplitude with gently ENE plunging axes (Fig. S3a). They are the result of nearly south–north-oriented shortening. Some D_2 folds are characterised by the presence of axial cleavage, further indicating nearly south–north-oriented compression. The D_3 folds refolded the F_2 axes and axial planes (Fig. S3a). They are open to tight, and have a decametric to hectametric wavelength and amplitude, with upright, or steeply inclined axial surfaces. Furthermore, the joints and cleavages across the Xishui-Renhuai area show marked dispersion (Fig. 3), which is consistent with multiphase deformations. Note that fold axes with moderate to high plunges of 30°–45° are

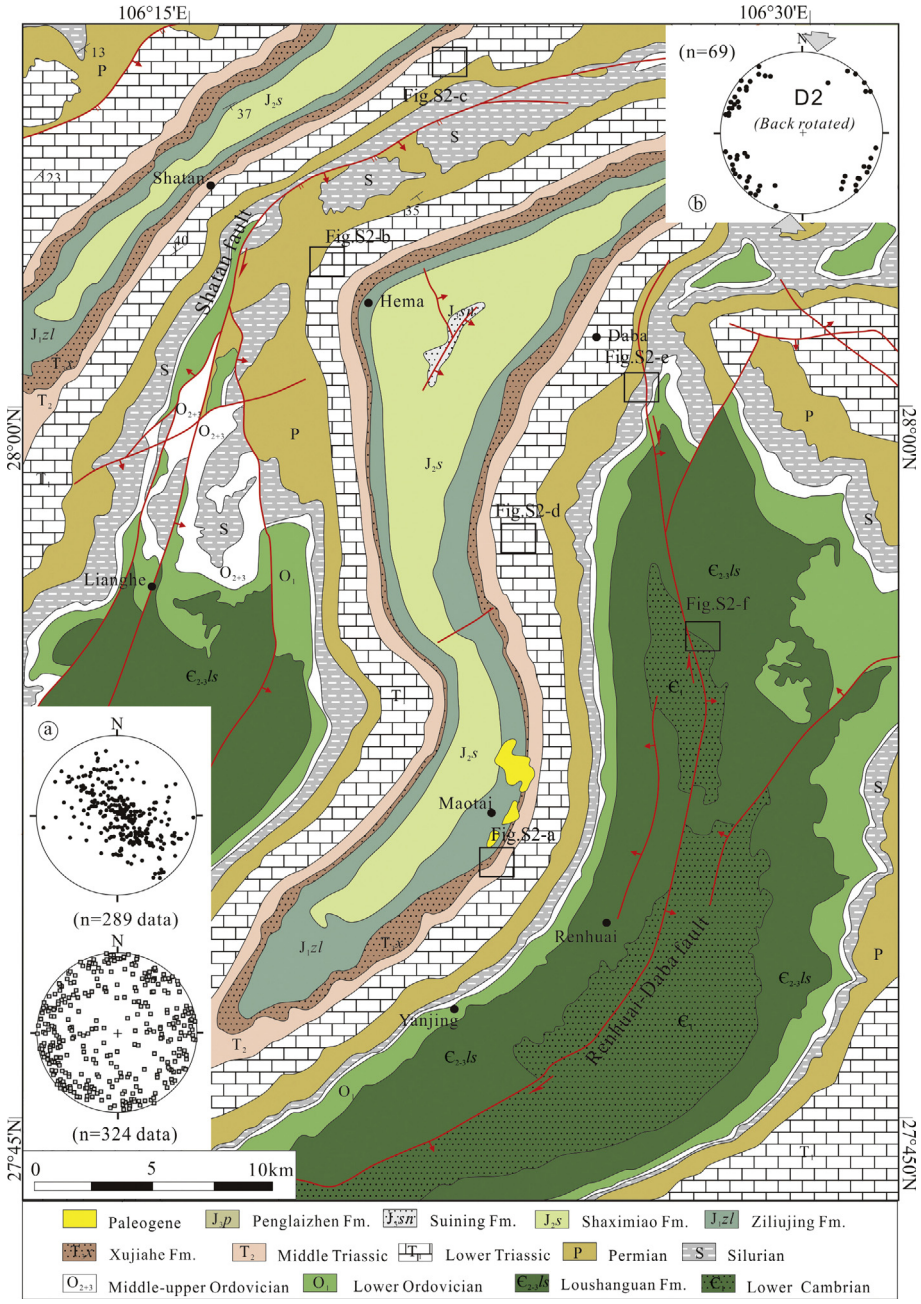

Fig. 3. (Color online) Detailed geologic map and representative structures of the middle Daloushan. (a) Dispersed stratification and cleavage in region. (b) Back-rotated conjugate joint sets, indicating south–north-oriented parallel-layer shortening (D_2).

dominant and distributed along a great circle in the Hema syncline (Fig. S3b). If considered in combination with parafolds, it suggests a NE–SW-oriented shortening with dextral transpression (D_3).

Three types of bedding-perpendicular joint sets were recognized at the middle Xishui-Renhuai region. The first type is widespread at the limbs of the box anticlines, represented by moderately to strongly dipping fault-slips due to the folding and parallel-layer shortening (Fig. S3c). After unfolding, it suggests a nearly east–west-oriented shortening (D_1). The second type is widespread in the Late Triassic to Cretaceous sequences; some have coevally rotated axial cleavage due to the subsequent deformation (D_3). After back-rotation, maximum palaeostress of the second type of joint sets indicates a NNE–SSW-oriented shortening (D_2; Fig. 3b). The third joint set is not a significant feature in the outcrops. It is locally developed with the cleavage of D_3 folds, under a nearly NE–SW-oriented shortening. A distinct cross-cutting relation between the cleavage and joints of D_3 folds and the second bedding-perpendicular joint set (Fig. S3d) suggests that this is the youngest set.

The middle Xishui-Renhuai area is associated with widespread northeast-striking dextral faults characterized by west- to northwest-thrusting (Fig. S1). To the north, the fault (e.g., the Renhuai-Daba fault) is linked with at least two branches. The slickensides on these branches indicate that dextral transpression and northwestward thrusting occurred under a NW–NNW oriented shortening (D_2) (Fig. S3e). To the south, low-angle, plunging parafolds characterize the Renhuai Fault. The pervasive axial cleavage of these folds are cut and rotated by the thrust fault (Fig. S3f).

3.3. Western Weixin-Yanjin area

Widespread superimposed folds are present in the western segment of the Daloushan and are concentrated in the Weixin area. The D2 folds are dominant, with similar folds having westward plunging axes and nearly upright inclined axial planes. The D3 folds are open to tight, with NW-to-NNW- and upright-plunging axes, or steeply inclined axial surfaces, indicating that ENE-to-NE-oriented shortening (D3) occurred in this area. The D3 folding usually refolded the D2 structures (i.e. F2 axis and axial plane) and resulted in parafolds in the outcrops (Fig. S4a), and dispersed stratification and cleavage across the western Daloushan (Fig. 4a). The bedding attitude in the Permian strata suggests a low-angle intersection between two axes (i.e. F3 to F2 axes) (Fig. S4b), which could be related to the rotation of superimposed deformation.

Two types of bedding-perpendicular joint sets are present in the western segment. The first set is widespread in the pre-Jurassic strata, with nearly south–north and east–west trends and moderate-to-high dips (Fig. 4b). Several of these joints cut the axial cleavage of the D2 folds, indicating a later D3 antiform. After unfolding, it suggests a NE–SW-oriented layer-parallel shortening (D3) (Fig. 4b; Fig. S2c). The second joint set is widespread in low-angle to sub-horizontal Permian to Cretaceous sequences. Maximum stresses of conjugated joints suggest a NW–SE-oriented shortening (Fig. S4e). There is no evidence that axial planar cleavage development and folds are related to this bedding-perpendicular joint set. Moreover, this set cuts most of the other joints, and thus, we deduce that it is the youngest in the Daloushan (D4).

The western segment has been affected by ENE striking and southward thrusting faults (Fig. S1). To the west, the thrust fault (e.g., Weixing-Mangbu fault) places northwest-dipping Silurian–Cambrian strata over southeast-dipping Cambrian strata, indicating southeastward thrusting. To the east, the Weixin Fault dips to the north and places low-angle dipping Silurian strata above the northwest-dipping Permian strata. Slickensides indicate dextral transpression and S-vergent thrusting occurred under a NW–NNW-oriented shortening (D_4).

4. Thermochronological results

To constrain the timing and magnitude of deformation and exhumation across this range, 15 apatite fission-track (AFT) samples have been analysed (Fig. 1, Table S1). All AFT ages are scattered, ranging from 27 Ma to 60 Ma, with lengths ranging from 10.7 μm to 12.6 μm (Fig. 5). Time–temperature histories of all samples were modelled using HeFTy, with an aim to:

- unravel the burial and exhumation histories across the Daloushan;
- test the coupling relation between deformation (and/or erosional processes) and the cooling event.

Representative thermal histories are shown in Fig. 5. Most thermal histories (e.g., ACQ1) from the Daloushan indicate that following the deposition, they reached their maximum burial depth at ~80 Ma. These samples show a continuous slow cooling rate of 0.5 °C–0.8 °C/Ma, with an acceleration of 2 °C–3 °C/Ma during the last 20–10 Ma. Furthermore, samples BS022, BS040 and PD048 located in the eastern Daloushan show a rapid cooling rate from 80 to 60 Ma, followed by a rapid cooling at ~5 Ma, with rates of 4 °C–5 °C/Ma. Some samples (e.g., XW022) in the western Daloushan show a rapid cooling rate through ~110 °C at 40–30 Ma, followed by an acceleration of ~4 °C/Ma during the last ~10 Ma. These relatively slow and rapid cooling rates correspond to exhumation rates of ~0.03 and ~0.1 mm/yr, when considering a geothermal gradient of ~30 °C/km and a surface temperature of ~15 °C (BGMRSP, 1991). The AFT data thus identified four periods of exhumation at the Daloushan:

- burial history prior to the Late Cretaceous (~80 Ma);
- low-rate exhumation during the Palaeogene;
- local increase to high-to-rapid exhumation rates at 40–30 Ma;
- significant increase in exhumation starting at 20–5 Ma.

5. Post-Late Mesozoic exhumation and deformation of the Daloushan

5.1. D1–D2 deformations

The deformed Upper Cretaceous red-bed sequences are widespread in the southern Sichuan Basin, where they are

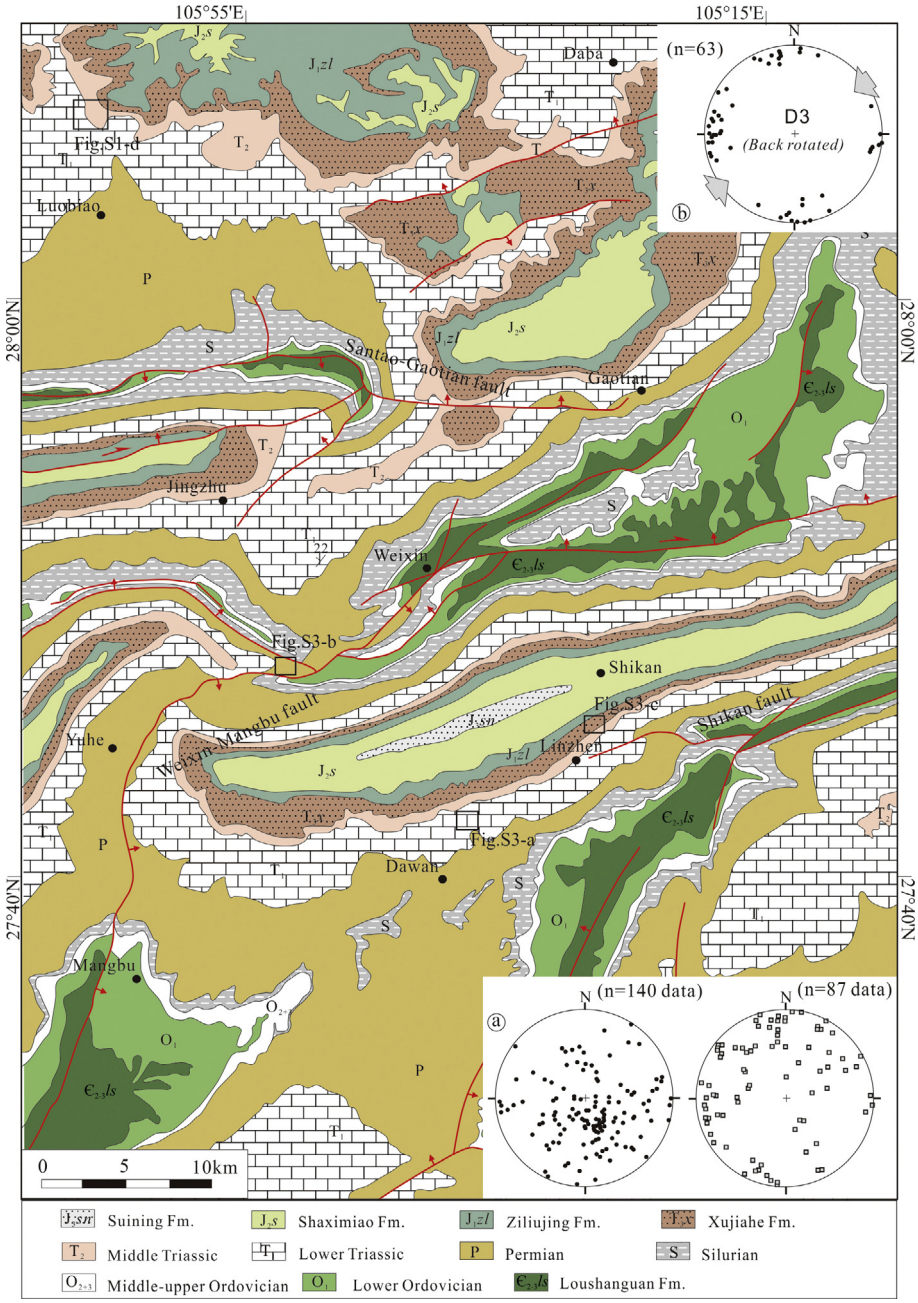

Fig. 4. (Color online) Detailed geologic map and representative structures of the western Daloushan. (a) Dispersed stratification and cleavage in region. (b) Back-rotated conjugate joint sets, indicating NE–SW-oriented parallel-layer shortening (D_3).

overlain by undeformed Lower Cenozoic strata (Fig. 1c, Fig. 3). Although the occurrence of Lower Cenozoic rocks is restricted, it indicates that the main phase of deformation affecting the Daloushan occurred at post-Late Cretaceous to Early Cenozoic times. This is supported by widespread low-rate post-burial cooling of the AFT samples across the Sichuan Basin (Deng et al., 2013). Note that the superimposition of D_2 over D_1 folds is recognized in the eastern Daloushan, while D_3 over D_2 folds are widespread in the middle and western segments. Thus, we argue that the D_1 east–west-oriented shortening was a pre-main phase deformation and occurred at the end of the Early Cretaceous, affecting the eastern Daloushan (Fig. 5A). Five factors support this argument:

- west- to NW-vergent thrusts and folds in the eastern Daloushan;
- a northwestward thrusting with shortening of ~80–100 km that predominantly occurred in the Late Jurassic–Early Cretaceous, related to the Xuefeng Orogeny (Li et al., 2012a, 2012b, 2012c; Mei et al., 2010; Yan et al., 2003);

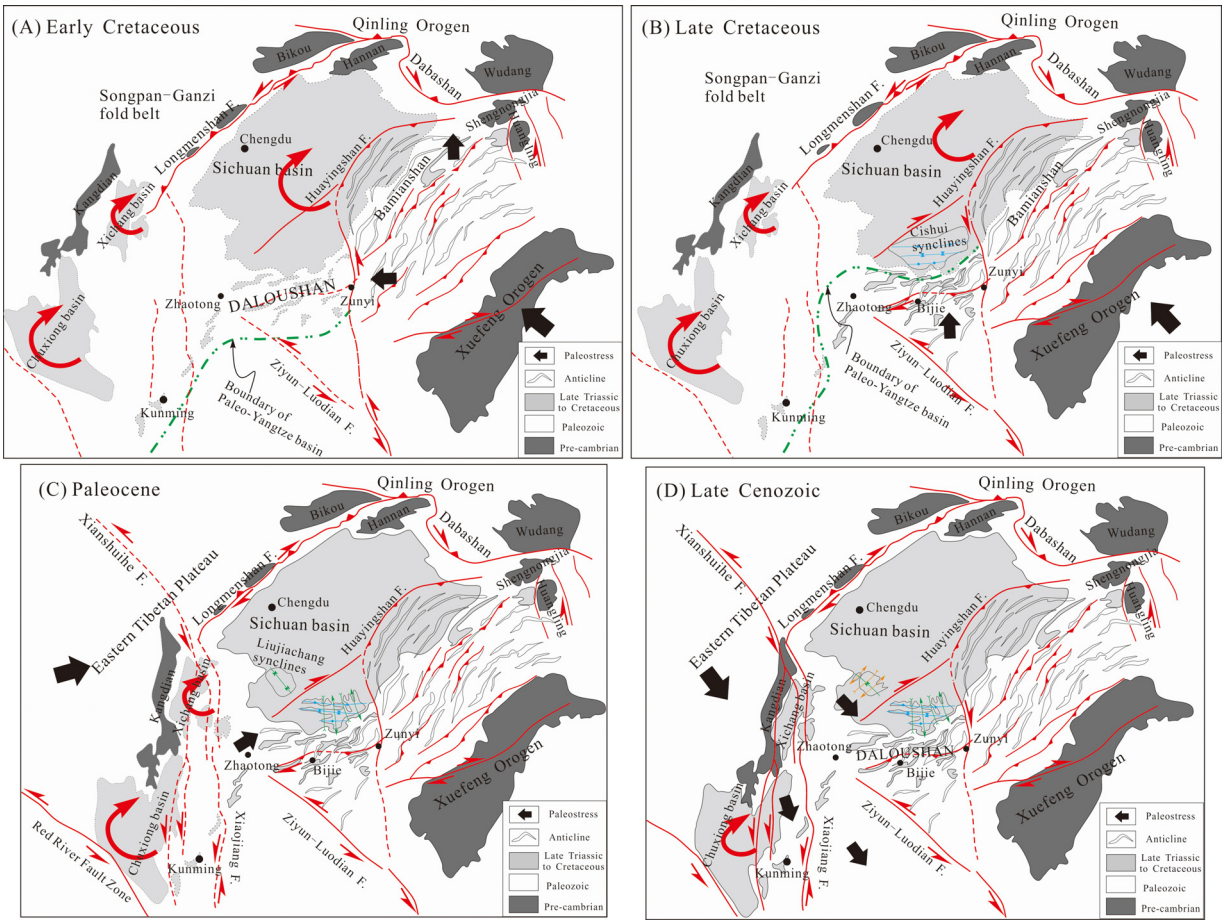

Fig. 5. (Color online) Schematic reconstruction of the Daloushan. (A) At the end of Early Cretaceous, the eastern Daloushan was subject to a west- to NW-vergent-oriented shortening deformation. (B) In the Late Cretaceous (~80 Ma), the main phase deformation of the Daloushan shows south–north-oriented shortening affected by the diachronous deformation of the Xuefeng Orogen combined with sinistral strike-slipping at the Ziyun-Luodian Fault. (C) In the Paleogene (40–20 Ma), the Daloushan was subject to NE–SW-oriented shortening under a far-field effect of the Indo-Asia collision; during this time, substantial clockwise rotation and an offset occurred across the southeastern margin of Tibetan Plateau, in particular at the Chuxiong and Xichang Basins. (D) Late Cenozoic (10–5 Ma) NE–SW-oriented shortening deformation, showing a close relationship with the eastern growth of the Tibetan Plateau, which led to the final establishment of the southern margin of the Sichuan Basin.

- a moderate-to-high angle unconformity between the K_2/K_1 in the Yuanma Basin, located southeast away from the Daloushan (Li et al., 2012a, 2012b, 2012c);
- a widespread para-unconformity between the K_2/K_1 across the southern Sichuan Basin;
- a pre-main phase folding affecting Early Cretaceous rocks also recognized in other areas of the Yangtze Block, e.g., the Yuanma Basin (Li et al., 2012a, 2012b, 2012c) and the South China Block (Wang et al., 2013).

In the southwestern Sichuan Basin, there is an obvious change in depositional contact between Late Cretaceous and Early Cenozoic strata, shown by decreasing angularity at the unconformity from south to north (Deng et al., 2012). After that time, all samples from the Sichuan Basin and the Daloushan experienced slow cooling and uplift during the Palaeogene. This is consistent with a gentle deformation of the Upper Cretaceous across the southern Sichuan Basin. Thus, we consider ~80 Ma to be the time of the main phase deformation of the Daloushan (D_2). Such south–north-oriented deformations were recognized across the Yangtze Block, e.g., the southeastern Sichuan, the Yuanma and Badong basins (Li et al., 2012a, 2012b, 2012c; Liu et al., 2012), showing a close correlation with the Xuefeng orogen.

At the end of the Early Cretaceous, a northwestward-oriented thrusting of the Xuefeng Orogen affected the Yangtze Block, with a shortening of ~80–100 km (Fig. 5). The curved Bamianshan structural belt in the southeastern Sichuan Basin formed along the Huayingshan and Nanchuan-Zunyi faults during this time, with only ~10 km of shortening (Mei et al., 2010). It resulted in the reactivation of the Nanchuan-Zunyi Fault to accommodate a nearly east–west-oriented shortening (D_1) (Fig. 5A). However, the Sichuan Basin suffered only minor clockwise rotation in this time, as indicated by the palaeomagnetism of Cretaceous to Lower Tertiary rocks (Huang and Opdyke, 1992). This is consistent with most parts of its northern and western margins, which show no significant shortening and displacement (Liu et al., 2012; Roger et al., 2010).

During the Late Cretaceous, northwestward thrusting of the Xuefeng Orogen was backstopped by the rigid basement of the Sichuan Basin to accommodate south–north-oriented compression in middle and western segments of the Daloushan, with strike-slipping at the Ziyun-Luodian Fault (D_2; Fig. 5B). This resulted in an initial exhumation across the Daloushan due to shortening less than ~10–20 km. Thus, we suggest that the Daloushan corresponds to the geodynamics of the Xuefeng Orogen during D_2 deformation, which is related to the westward subduction of the Pacific Plate (Wang et al., 2013; Yang, 2013). The latter event recorded in the South China block is supported by the widespread occurrence of I-, S- and A-type granites and volcanic rocks, with an age span of ~80–110 Ma.

5.2. D3–D4 deformations

AFT data suggest that rapid uplift and cooling to the closure temperature occurred from 40 to 30 Ma in the western Daloushan and from 20 to 5 Ma in the eastern Daloushan. An Early Cenozoic red bed series locally outcrops in the southern Sichuan Basin, which experienced gentle deformation and erosion resulting in an angular unconformity between the Paleogene and Neogene strata. It indicates that deformation and exhumation occurred during the post-Late Palaeogene to Neogene (D_3).

Li et al. (2012a, 2012b, 2012c) and Deng et al. (2013) argued that major regional erosion across the Sichuan Basin started not earlier than 40–20 Ma, roughly later than the major plate reorganization of the Indo–Eurasia blocks (Najman et al., 2010). The latter resulted in large-scale Tibetan crustal mass movement eastward, and development of numerous lithospheric-scale strike-slip faults and shortening, etc. (Royden et al., 2008; Tapponnier et al., 2001). From the Red River fault zone in the south to the Xianshuihe fault in the north, the shear distance and offset that occurred during Palaeocene times decrease from ~300 km to ~40 80 km (Leloup et al., 1995; Wang et al., 1998). Furthermore, the process accommodated substantial clockwise rotation, e.g., the Chuxiong Basin with a rotation of 40°–30° and the Xichang Basin with a rotation of 10°–5°, as indicated by Late Cretaceous to Tertiary palaeomagnetic data (Sato et al., 2001). Note that the NE–SW-oriented deformation is recognized across the eastern margin of the Tibetan Plateau and the upper Yangtze Block, e.g., Songpan-Ganze, the Sichuan Basin and the Badong Basin (Li et al., 2012a, 2012b, 2012c; Liu et al., 2012; Wilson et al., 2006). Thus, we suggest that the Late Palaeogene (40–20 Ma) represents the D_3 deformation of the Daloushan, related to NE–SW-oriented shortening (D_3, Fig. 5C). In the Late Palaeogene, the Daloushan experienced eastward migrating low-rate uplift and cooling. Such a deformation resulted in significant south-vergent thrusting, with some shortening along the western Daloushan.

Although there was a low-rate erosional process in the Palaeogene, most samples show a relatively rapid cooling rate of 0.1 mm/year at 20–10 Ma, in particular in the western Daloushan. During this time, rapid cooling and exhumation occurred at the eastern margin of the Tibetan Plateau (Deng et al., 2015; Li et al., 2012a, 2012b, 2012c). However, the clockwise rotation and offset was much smaller than those that occurred during the Palaeocene, a $< 5^\circ$ rotation at the Chuxiong Basin, as indicated by palaeomagnetic data (Li et al., 2013), a minor rotation, with ~10–20 km offset and shortening across the Daliangshan (Wang et al., 1998). To the east of the Daloushan, most samples show rapid cooling and uplift at ~5 Ma. An eastward propagation of geodynamic forcing should thus be invoked to explain eastward migration of rapid cooling and changes in the unconformity across the southern Sichuan Basin. It resulted in rapid cooling and uplift at 20–10 Ma, with a moderate-to-high angle unconformity developing between Neogene strata and its overlain sequence across the southwestern Sichuan Basin. To the east, a rapid cooling and uplift occurred at ~5 Ma, with a low-angle unconformity to paraconformity developing in the southeastern Sichuan Basin (BGMRSP, 1991; Deng et al., 2012). Therefore, we conclude that most of the uplift and exhumation associated with the NW–SE oriented shortening in the Daloushan occurred during the last 20–5 Ma (D_4, Fig. 5D). It is result of the eastern growth of the Tibetan plateau causing widespread regional deformation (Roger et al., 2010; Wilson et al., 2006).

The Daloushan, where four post-Late Mesozoic regional events have been recognized, exhibit a changing geodynamics regime (Fig. 5). It is considered to be the result of northwestward thrusting during the Xuefeng Orogeny, part of the Palaeo-Pacific Tectonic Domain (D_1–D_2) and of eastward growth of the Tibetan Plateau, belonging to the Tethys–Himalayan Domain (D_3–D_4). Therefore, this indicates that a change in the tectonic regime occurred in the centre of the Yangtze Block, after the D_2 deformation. Such a change in tectonism could accommodate the reversion of strike-slip faults around the Sichuan Basin, e.g., the Longmenshan fault, Nanchuan-Zunyi fault etc. (Liu et al., 2013 and reference therein). Thus, intracontinental strike-slipping faults that developed around the Daloushan and the Sichuan Basin represent the crustal response to the far-field effects of regional geodynamics (e.g., Leloup et al., 1995; Tapponnier et al., 2001).

6. Conclusions

The Daloushan mountain chain can be separated into two structural domains: an eastern domain governed by west- to NW-vergent thrusting, and a western domain with south-vergent thrusting. A close relationship between stratigraphy, multiphase deformation and modelled time-temperature histories have revealed four phases of kinematic evolution in the Daloushan:

- Early-Late Cretaceous east–west-oriented compression (D_1);
- Late Cretaceous (~80 Ma) nearly south–north-oriented compression (D_2);
- Late Palaeogene (40–20 Ma) NE–SW-oriented compression (D_3) and (4) Late Cenozoic (10–5 Ma) NW–SE oriented shortening (D_4).

Therefore, the Daloushan is considered to be the result of multiphase shortening in response to the northwestward thrusting of the Xuefeng Orogen, belonging to the Palaeo-Pacific Tectonic Domain (D_1–D_2). The tectonics has been modified by the eastward growth of the Tibetan Plateau, related to the Tethys-Himalayan Domain (D_3–D_4). This demonstrates that a change in intra-continental tectonic forcing occurred in the centre of the Yangtze Block after the D_2 deformation (post-Late Cretaceous).

Acknowledgments

This work was supported by National Basic Research Program of China (No. 2012CB214805), and NSFC (Nos. 41402119, 2014JQ0057, 41472107). We acknowledge Jerome van der Woerd, Gweltaz Mahéo, and Editor Isabelle Manighetti for their comments and suggestions that helped us to improve the manuscript. We are thankful to Frank Thomas for assistance with English.

Appendix A. Supplementary data

Supplementary data associated with this article can be found, in the online version, at http://dx.doi.org/10.1016/j.crte.2015.06.009.

References

Bureau of Geology and Mineral Resources of Sichuan Province (BGMRSP), 1991. Regional Geology of Sichuan Province. Geological Publishing House, Beijing1–735.

Deng, B., Liu, S.G., Enkelmann, E., Li, Z.W., Ehlers, T., Jansa, L., 2015. Late Miocene accelerated exhumation of the Daliang Mountains, southeastern margin of the Tibetan Plateau. Int. J. Earth Sci. 104, 1061–1081.

Deng, B., Liu, S.G., Li, Z.W., Cao, J.X., Sun, W., 2012. Late Cretaceous Tectonic change of the eastern Margin of Tibetan Plateau. Results from Multi-system Thermochronology. J. Geol. Soc. India 80, 241–254.

Deng, B., Liu, S.G., Li, Z.W., Liu, S., Wang, G.Z., Sun, W., 2013. Differential Exhumation in the Sichuan Basin, eastern Margin of Tibetan Plateau, from Apatite Fission-track Thermochronology. Tectonophysics 951, 98–115.

Hsu, K.J., Li, J., Cheng, H., Wang, Q., Sun, S., Sengor, A.M.C., 1990. Tectonics of South China: Key to understanding West Pacific geology. Tectonophysics 183, 9–39.

Huang, K.N., Opdyke, N.D., 1992. Paleomagnetism of Cretaceous to Lower Tertiary rocks from southwestern Sichuan: a revisit. Earth Planet. Sci. Lett. 112, 29–40.

Judge, P., Allmendinger, R.W., 2013. Assessing uncertainties in balanced cross sections. J. Struct. Geol. 33, 458–467.

Lacassin, R., Scharer, U., Leloup, P.H., Arnaud, N., Tapponnier, P., Liu, X.H., Zhang, L.S., 1995. Tertiary deformation and metamorphism SE of Tibet: The folded Tiger-leap decollement of NW Yunnan, China. Tectonics 15, 605–622.

Leloup, P.H., Lacassin, R., Tapponnier, P., Scharer, U., Zhong, D.L., Liu, X.H., Zhang, L.S., Ji, S.C., Trinh, P.T., 1995. The Ailao Shan-Red River shear zone (Yunnan, China). Tertiary transform boundary of Indochina. Tectonophysics 251, 3–84.

Li, J.H., Zhang, Y.Q., Dong, S.W., Li, H.L., 2012c. Late Mesozoic–Early Cenozoic deformation history of the Yuanma Basin, central South China. Tectonophysics 570–571 163-183.

Li, S.H., Deng, C.L., Yao, H.T., Huang, S., Liu, C.Y., He, H.Y., Pan, Y.X., Zhu, R.X., 2013. Magnetostratigraphy of the Dali Basin in Yunnan and implications for late Neogene rotation of the Southeast margin of the Tibetan Plateau. J. Geophys. Res.: Solid Earth 118, 791–807.

Li, S.Z., Santosh, M., Zhao, G.C., Zhang, G.W., Jin, C., 2012b. Intracontinental deformation in a frontier of super-convergence. A perspective on the tectonic milieu of the South China Block. J. Asian Earth Sci. 49, 313–329.

Li, Z.X., Li, X.H., 2007. Formation of the 1300-km-wide intracontinental orogen and postorogenic magmatic province in Mesozoic South China. A flat-slab subduction model. Geology 35, 179–182.

Li, Z.W., Liu, S.G., Chen, H.D., Deng, B., Hou, M.C., Wu, W.H., Cao, J.X., 2012a. Spatial variation in Meso-Cenozoic exhumation history of the Longmen Shan thrust belt (eastern Tibetan Plateau) and the adjacent western Sichuan basin. Constraints from fission-track thermochronology. J. Asian Earth Sci. 47, 185–203.

Liu, S.G., Deng, B., Li, Z.W., Jansa, L., Liu, S., Wang, G.Z., Sun, W., 2013. Geological Features and Evolutionary Processes of the Longmenshan Intracontinental Composite Orogen in eastern Margin of the Tibetan Plateau. J. Earth Sci. 24, 874–890.

Liu, S.G., Deng, B., Li, Z.W., Sun, W., 2012. Architectures of Basin-Mountain Systems and Their Influences on Gas Distribution, A Case Study from Sichuan Basin, South China. J. Asian Earth Sci. 47, 204–215.

Mei, L.F., Liu, Z.Q., Tang, J.G., Shen, C.B., Fan, F.F., 2010. Mesozoic Intra-Continental progressive deformation in western Hunan-Hubei-eastern Sichuan Provinces of China, evidence from apatite fission track and balanced cross-section. Earth Sci. J. China University Geosci. 35, 161–174.

Najman, Y., Appel, E., Boundagher-Fadel, M., Bown, P., Carter, A., Garzanti, E., Godin, L., Han, J.T., 2010. Timing of India-Asia collision: Geological, biostratigraphic, and palaeomagnetic constraints. J. Geophys. Res. 115, B12614, http://dx.doi.org/10.1029/2010JB007673.

Roger, F., Jolivet, M., Malavieille, J., 2010. The tectonic evolution of the Songpan-Garze (North Tibet) and adjacent areas from Proterozoic to Present. A synthesis. J. Asian Earth Sci. 39, 254–269.

Royden, L.H., Burchfiel, B.C., van der Hilst, R.D., 2008. The geological evolution of the Tibetan Plateau. Science 321, 1054–1058.

Sato, K., Liu, Y.Y., Zhu, Z.C., Yang, Z.Y., Otofuji, Y., 2001. Tertiary paleomagnetic data from northwestern Yunnan. China: further evidence for large clockwise rotation of the Indochina block and its tectonic implications. Earth Planet. Sci. Lett. 185, 185–198.

Tapponnier, P., Xu, Z.Q., Roger, F., Meyer, B., Arnaud, N., Wittlinger, G., Yang, J.S., 2001. Oblique stepwise rise and growth of the Tibet Plateau. Science 294, 1671–1677.

Wang, E.Q., Burchfiel, B.C., Royden, L.H., Chen, L., Chen, J., Li, W., Chen, Z., 1998. Late Cenozoic Xianshuihe-Xiaojiang, Red River, and Dali fault systems of southwestern Sichuan and central Yunnan, China: Boulder, Colorado. Geol. Soc. America Special Paper 327, 1–108.

Wang, Y.J., Fan, W.M., Zhang, G.W., Zhang, Y.H., 2013. Phanerozoic tectonics of the South China Block. Key observations and controversies. Gondwana Res. 23, 1273–1305.

Wilson, C.J.L., Harrowfield, M.J., Reid, A.J., 2006. Brittle modification of Triassic architecture in eastern Tibet, implications for the construction of the Cenozoic plateau. J. Asian Earth Sci. 27, 341–357.

Yan, D.P., Zhou, M.F., Song, H.L., Wang, X.W., Malpas, J., 2003. Origin and tectonic significance of a Mesozoic multi-layer over-thrust system within the Yangtze Block (South China). Tectonophysics 36, 239–254.

Yang, Y.T., 2013. An unrecognized major collision of the Okhotomorsk Block with East Asia during the Late Cretaceous, constraints on the plate reorganization of the Northwest Pacific. Earth Sci. Rev. 126, 96–115.